# Modelling of gas-liquid reactors - stability and dynamic behaviour of a hydroformylation reactor, influence of mass transfer in the kinetics controlled regime

Elk, E.P. van; Borman, P.C.; Kuipers, J.A.M.; Versteeg, G.F.

*Published in:*
Chemical Engineering Science

*DOI:*
10.1016/S0009-2509(00)00375-4



*Publication date:*
2001

PERGAMON

Chemical Engineering Science 56 (2001) 1491–1500

Chemical Engineering Science

www.elsevier.nl/locate/ces

# Modelling of gas–liquid reactors — stability and dynamic behaviour of a hydroformylation reactor, influence of mass transfer in the kinetics controlled regime

E. P. Van Elk[a,*], P. C. Borman[b], J. A. M. Kuipers[c], G. F. Versteeg[c]

[a]*Procede Twente BV, P.O. Box 217, 7500 AE Enschede, Netherlands*
[b]*DSM Research, P.O. Box 18, 6160 MD Geleen, Netherlands*
[c]*Department of Chemical Engineering, Twente University of Technology, P.O. Box 217, 7500 AE Enschede, Netherlands*

**Abstract**

On behalf of the development of new hydroformylation reactors, a research project was initiated to examine the dynamics of hydroformylation processes. The current paper presents the results of applying the rigorous reactor model (van Elk et al., Chem. Engng. Sci. 45 (1999) 4869–4879; Chem. Engng. J. 76 (2000) 223–237) and the approximate reactor model (van Elk et al., 1999) on a new, to be developed, hydroformylation reactor with complex kinetics. The reaction considered is of the first order in the olefin and the catalyst concentration, while the apparent reaction order in hydrogen varies between 0 and 1 and in CO between $-1$ and 1, depending on the hydrogen and carbonmonoxide concentrations, respectively. The influence of the cooler design and the mass transfer on the dynamic behaviour is investigated in the kinetic controlled regime. It is shown that this reactor will show oscillatory behaviour under certain realistic operating conditions. From stability analysis, it was found that the desired steady state (temperature, conversion) exists for a wide range of mass transfer parameters. However, the cases are only statically similar, but dynamically show an important difference: for some conditions, the steady state is found to be dynamically stable, while for others the same steady state is found to be dynamically unstable (limit cycle). This unusual phenomenon is possible due to the negative reaction order in CO. 

*Keywords:* Hydroformylation reactor model; Dynamic stability; Limit cycle; Bifurcation analysis; Design rules

## 1. Introduction

With respect to the development of a new hydroformylation reactor, a research project was initiated to examine the dynamics of hydroformylation processes. The dynamic behaviour of a reactor in general and especially of a hydroformylation reactor is a very important part of the reactor design. A literature survey indicated that undesired sustained temperature oscillations may exist in hydroformylation reactors under certain circumstances (Vleeschhouwer, Garton, & Fortuin, 1992). In plant operation, these conditions have to be avoided because they may adversely affect product quality, catalyst degradation and downstream operations and can lead to serious difficulty in process control and unsafe reactor operations. Two models to be used as design tools have been developed and validated: (1) A rigorous reactor model (van Elk, Borman, Kuipers, & Versteeg, 1999, 2000) and (2) an approximate reactor model for stability analysis (van Elk et al., 1999). The models are used to investigate the influence of the cooler design and the mass transfer coefficient and/or contact area on the stability and dynamic behaviour of the reactor.

The rigorous model (van Elk et al., 1999, 2000) requires a minimum amount of model assumptions and simplifications; moreover, it takes all relevant phenomena into account. The rigorous model is based on the following major assumptions:

1. The mass transfer in the gas phase is described with the stagnant film model.

* Corresponding author. Tel.: +31-53-4894480; fax: +31-53-4894774.
*E-mail address:* edwin.vanelk@procede.nl (E. P. van Elk).

0009-2509/01/$ - see front matter 
PII: S0009-2509(00)00375-4

2. The mass transfer in the liquid phase is described with the Higbie (1935) penetration model.
3. The contact time according to the penetration model is small compared to the liquid-phase residence time.
4. Both the gas and the liquid phase are assumed to be perfectly mixed (i.e. CISTRs).

The approximate model (van Elk et al., 1999) is a much simpler one based on some additional assumptions. This model takes only the key phenomena into account. The model consists of liquid-phase material balances (ordinary differential equations) and an approximate algebraic expression for the enhancement factor. The approximate model is based on the following additional assumptions:

1. The influence of mass transfer is sufficiently accurate described by an approximate and explicit analytical expression for the enhancement factor ($E_a$).
2. The influence of temperature profiles on micro scale can be neglected.
3. The resistance to mass transfer in the gas-phase can be neglected.
4. The influence of the gas-phase heat balance can be neglected or alternatively the gas- and liquid-phase heat balances can be combined into one overall heat balance.
5. The gas-phase concentration is constant or alternatively the gas-phase partial pressure is constant. This assumption is fulfilled when a sufficiently fast partial pressure regulation is present.

The approximate model is very useful to create stability maps from which design rules for stable operation can be obtained. Using the more accurate rigorous model as a final check-up for the chosen set of operating conditions is however recommended.

Illustrative examples (van Elk et al., 1999) showed that for fictitious gas–liquid reactors, with simple first- or second-order kinetics, operating conditions can be created where oscillations (limit cycles) are found. It was also shown that the approximate model is a very useful tool for predicting the regions where instabilities take place and more important to find design rules which ensure stable operations.

The current study presents the results of applying both the rigorous and the approximate reactor model on a hydroformylation process with more complex kinetics. It is shown that this reactor will show oscillatory behaviour under certain realistic operating conditions. The current study thus shows that limit cycles can be expected to exist for real industrial designs and not only for fictitious non-existing reactors and/or processes.

## 2. Theory

### 2.1. Introduction

Hydroformylation is a chemical process in which the addition of hydrogen and carbonmonoxide to an olefinic double bond takes place. The product is a mixture of normal- and iso-aldehyde and alcohols. The hydroformylation reaction is catalysed homogeneously by Group VIII metals (e.g. Ir, Co, Rh). The introduction of various ligands to the catalyst (e.g. $Co_2(CO)_6[P(n\text{-}C_4H_9)_3]_2$) and the operating conditions (i.e. pressure, temperature and $CO/H_2$-ratio) can have a significant influence on the selectivity.

The problem considered is a gas–liquid hydroformylation reactor with mass transfer of hydrogen and carbonmonoxide, followed by an irreversible reaction of complex kinetics:

$$H_2(g) + CO(g) + \text{olefine(l)} \rightarrow \text{aldehyde(l)}. \quad (1)$$

The complex kinetics equation used in this study is

$$R = k_{R0} e^{-E_{act}/RT}[\text{olefin}][\text{catalyst}] \frac{[H_2]}{(1 + K_{H_2}[H_2])} \frac{[CO]}{(1 + K_{CO}[CO]^2)}. \quad (2)$$

Thus, the reaction is assumed to be first order in the olefin and catalyst concentration, while the apparent reaction order in $H_2$ can vary between 0 and 1 and in CO between $-1$ and 1, depending on the hydrogen and carbonmonoxide concentrations, respectively.

Due to e.g. economical and technical reasons for the reactor design the following design constraints are assumed:

1. Total gas-phase pressure about 10 bar.
2. Molar $H_2$/CO-ratio in gas-phase near unity.
3. Operating temperature of about 100°C.
4. Catalyst concentration of 0.5 mol/m$^3$.
5. Conversion of about 50%.
6. Mass transfer rate ($k_l a$) between 0.025 and 0.2 s$^{-1}$.
7. Cooling capacity $UA$ and cooling temperature $T_{cool}$ to be determined for stable operation.

The chosen kinetic data and operating conditions of the reactor are representative for a family of hydroformylation processes.

### 2.2. Rigorous model

The rigorous reactor model as described by van Elk et al. (1999, 2000) considers all species on micro as well as on macro scale. However, over 99% of the calculation time is required for the micro scale model (i.e. the Higbie penetration model). To reduce the required calculation time almost by a factor two it was decided to include only

species $H_2$, CO and olefin in the micro model used for the hydroformylation reactor model. The other species and parameters (i.e. temperature, aldehyde and catalyst) are considered on the macro scale only. This simplification is allowed for this specific hydroformylation process provided that:

1. The influence of the temperature profile on micro scale is negligible due to a good heat transfer between the gas and the liquid phase.
2. The reaction is irreversible, so that the aldehyde concentration does not influence the reaction rate.
3. The catalyst concentration will be constant all over the reactor on micro as well as on macro scale.

The micro model for the phenomenon of mass transfer accompanied by a chemical reaction is thus governed by the following equations:

$$\frac{\partial[H_2]}{\partial t} = D_{H_2}\frac{\partial^2[H_2]}{\partial x^2} - R, \tag{3}$$

$$\frac{\partial[CO]}{\partial t} = D_{CO}\frac{\partial^2[CO]}{\partial x^2} - R, \tag{4}$$

$$\frac{\partial[olefin]}{\partial t} = D_{olefin}\frac{\partial^2[olefin]}{\partial x^2} - R. \tag{5}$$

To permit a unique solution of the non-linear partial differential equations (3) to (5) one initial (6) and two boundary conditions (7) and (8) are required:

$$t = 0 \text{ and } x \geqslant 0: \quad [i] = [i]_{l,bulk},$$
$$\text{where } i = H_2, CO, olefin, \tag{6}$$

$$t > 0 \text{ and } x = \delta_p: \quad [i] = [i]_{l,bulk},$$
$$\text{where } i = H_2, CO, olefin, \tag{7}$$

$$J_{H_2} = -D_{H_2}\left(\frac{\partial[H_2]}{\partial x}\right)_{x=0} = k_g\left([H_2]_{g,bulk} - \frac{[H_2]_{x=0}}{m_{H_2}}\right),$$

$$J_{CO} = -D_{CO}\left(\frac{\partial[CO]}{\partial x}\right)_{x=0} = k_g\left([CO]_{g,bulk} - \frac{[CO]_{x=0}}{m_{CO}}\right), \tag{8}$$

$$\left(\frac{\partial[olefin]}{\partial x}\right)_{x=0} = 0.$$

The material and energy balances describing the system on macro scale are

$$\frac{d[H_2]_{g,bulk}}{dt} = \frac{[H_2]_{g,in} - [H_2]_{g,bulk}}{\tau_g} - \frac{J_{H_2}a}{\varepsilon_g}, \tag{9}$$

$$\frac{d[CO]_{g,bulk}}{dt} = \frac{[CO]_{g,in} - [CO]_{g,bulk}}{\tau_g} - \frac{J_{CO}a}{\varepsilon_g}, \tag{10}$$

$$\frac{dT_g}{dt} = \frac{T_{g,in} - T_g}{\tau_g} - \frac{h_{ov}a(T_g - T_l)}{\rho_g C_{P,g}\varepsilon_g}, \tag{11}$$

$$\frac{d[H_2]_{l,bulk}}{dt} = \frac{[H_2]_{l,in} - [H_2]_{l,bulk}}{\tau_l} + \frac{J_{H_2}a}{\varepsilon_l} - R_{bulk}, \tag{12}$$

$$\frac{d[CO]_{l,bulk}}{dt} = \frac{[CO]_{l,in} - [CO]_{l,bulk}}{\tau_l} + \frac{J_{CO}a}{\varepsilon_l} - R_{bulk}, \tag{13}$$

$$\frac{d[olefin]_{l,bulk}}{dt} = \frac{[olefin]_{l,in} - [olefin]_{l,bulk}}{\tau_l} - R_{bulk}, \tag{14}$$

$$\frac{d[aldehyde]_{l,bulk}}{dt} = \frac{[aldehyde]_{l,in} - [aldehyde]_{l,bulk}}{\tau_l} + R_{bulk}, \tag{15}$$

$$\frac{d[catalyst]_{l,bulk}}{dt} = \frac{[catalyst]_{l,in} - [catalyst]_{l,bulk}}{\tau_l}, \tag{16}$$

$$\frac{dT_l}{dt} = \frac{T_{l,in} - T_l}{\tau_l} + \frac{h_{ov}a(T_g - T_l)}{\rho_l C_{P,l}\varepsilon_l} - \frac{UA(T_l - T_{cool})}{\rho_l C_{P,l}\varepsilon_l V_R} - \frac{R\Delta H_R}{\rho_l C_{P,l}}. \tag{17}$$

The overall rigorous mathematical model combines the micro and macro model Eqs. (3)–(17) by simultaneously solving the micro and macro model. The macro model is coupled to the micro model by the boundary conditions. The exact numerical implementation is described and validated in detail elsewhere (van Elk et al., 2000).

### 2.3. Bifurcation analysis

Bifurcation analysis is an efficient technique that allows analysis of the static and dynamic stability of processes without having to solve completely the dynamic equations describing the system. Various authors (e.g. Huang & Varma, 1981a; Vleeschhouwer et al., 1992; Heiszwolf & Fortuin, 1997; van Elk et al., 1999) discuss the theory of bifurcation analysis applied on ideally stirred tank reactors.

A system is considered point-stable if, after a sufficiently small perturbation from the steady state, the system returns to its initial state (i.e. asymptotic damping or spiral point, see Fig. 1). If the slope condition is violated, the system shows static instability (extinction or ignition to a static stable point, see Fig. 1). If the dynamic condition is violated, the system shows dynamic instability (limit cycle, see Fig. 1).

If a stability map (like Fig. 3) is made with S-shaped curves of the loci of points representing the steady states

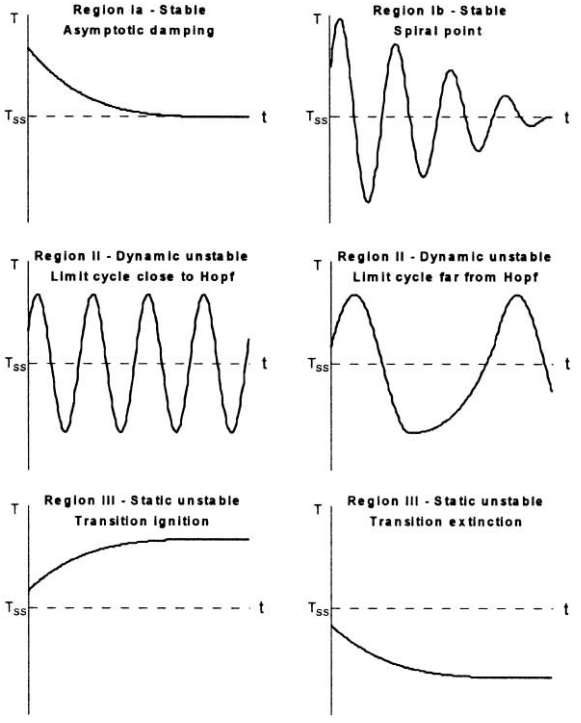


Fig. 1. Schematic presentation of various kinds of dynamic behaviour of a system after a step disturbance. The dotted horizontal line indicates the desired steady state.

of the system as a function of a certain parameter (for example the coolant temperature), two additional curves can be drawn to divide the figure into three distinct regions, each with a characteristic dynamic behaviour. The two curves are the fold bifurcation curve and the Hopf bifurcation curve. The three distinct regions are: I. region with point-stable steady states; II. region with dynamic instability (also called orbitally stable region or limit cycle region); III. region with static instability. Region I can be further divided in two separate regions by the double Eigenvalue curve (DEV). Region 1a shows asymptotic damping and region 1b spiral point behaviour. The dynamic behaviour of the system in each of the four regions is schematically shown in Fig. 1.

Application of the bifurcation analysis requires simplification of the rigorous reactor model to an approximate reactor model consisting of a system of ordinary differential and algebraic equations.

### 2.4. Approximate model (4 ODEs)

The rigorous reactor model is too complicated for a bifurcation analysis. Therefore, the rigorous reactor model must be simplified to an approximate model with only ordinary differential and algebraic equations. The simplest system of ODEs in agreement with the assumptions given in Section 1 is (assuming that the liquid feed is free of $H_2$ and CO):

$$\frac{d[H_2]_{l,bulk}}{dt} = -\frac{[H_2]_{l,bulk}}{\tau_l} + \frac{k_l E_{a,H_2} a}{\varepsilon_l}(m_{H_2}[H_2]_g - [H_2]_{l,bulk}) - R_{bulk}, \quad (18)$$

$$\frac{d[CO]_{l,bulk}}{dt} = -\frac{[CO]_{l,bulk}}{\tau_l} + \frac{k_l E_{a,CO} a}{\varepsilon_l}(m_{CO}[CO]_g - [CO]_{l,bulk}) - R_{bulk}, \quad (19)$$

$$\frac{d[olefin]_{l,bulk}}{dt} = \frac{[olefin]_{l,in} - [olefin]_{l,bulk}}{\tau_l} - R_{bulk}, \quad (20)$$

$$\frac{dT_l}{dt} = \frac{T_{l,in} - T_l}{\tau_l} - \frac{UA(T_l - T_{cool})}{\rho_l C_{P,l} \varepsilon_l V_R} - \frac{R\Delta H_R}{\rho_l C_{P,l}}. \quad (21)$$

The model requires an algebraic expression (AE) for the enhancement factors to replace the micro model. The fact that the micro and macro balances are no longer solved simultaneously makes the model an approximate model. van Swaaij and Versteeg (1992) concluded in their review that no generally valid approximate expressions are available to cover all gas–liquid processes accompanied with complex reactions. Only for some asymptotic situations these expressions are available. For the present study, it was found by the results of the rigorous model that for the conditions of interest the process is almost completely controlled by the reaction kinetics. In that case, the enhancement factors are approximately equal to unity:

$$E_{a,H_2} = E_{a,CO} \approx 1.0. \quad (22)$$

For hydroformylation or other processes (partly) controlled by mass transfer an approximate expression of the enhancement factor as a function of the liquid-phase concentrations and temperature is required.

Creating a stability map of the system described by Eqs. (18)–(22) by the analytical perturbation analysis is not possible. However, bifurcation software packages like LOCBIF or AUTO can create a stability map for the system using a numerical bifurcation technique. Implementation of Eqs. (18)–(22) in bifurcation software (LOCBIF) results in an easy to use prediction method. This method is very powerful for attaining design rules for stable operation of the hydroformylation reactor. LOCBIF is a software package that has the numerical routines to explore the existence and stability of equilibria in dynamic models.

### 2.5. Saturation and utilisation

Two additional dimensionless parameters will be used: the degree of saturation and the degree of utilisation of the liquid bulk. The degree of saturation of the liquid bulk is the ratio of the liquid-phase concentration to the liquid-phase concentration when the liquid phase is

saturated:

$$\eta_a \equiv \frac{[A]_{l,\mathrm{bulk}}}{[A]_{l,\mathrm{sat}}} \approx \frac{[A]_{l,\mathrm{bulk}}}{m_a[A]_g}. \quad (23)$$

For increasing reaction rate or decreasing mass transfer rate the degree of saturation will approach to a certain minimum (often zero) and for decreasing reaction rate or increasing mass transfer rate the degree of saturation will approach to a certain maximum.

The degree of utilisation of the liquid phase is the ratio of the actual conversion rate of a gas-phase component ($A$) to the conversion rate of $A$ that would occur if the entire reaction phase were in equilibrium with the interface:

$$\eta \approx \frac{\frac{1}{\theta}\int_0^\theta \xi_a \,\mathrm{d}t}{\int_0^\theta R_{a,\mathrm{sat}} \,\mathrm{d}t\, \varepsilon_l V_R}. \quad (24)$$

For increasing reaction rate or decreasing mass transfer rate the degree of utilisation will approach to a certain minimum (often zero) and for decreasing reaction rate or increasing mass transfer rate the degree of utilisation will approach to a certain maximum.

## 3. Results

### 3.1. Introduction

The rigorous model (Section 2.2) and the approximate model (Section 2.4) are applied on the hydroformylation process described in Section 2.1. The system parameters are given in Table 1 (kinetic and physical data) and Table 2 (fixed operating conditions). The process has three adjustable parameters ($k_la$, $UA$, $T_{\mathrm{cool}}$) and because the reactor temperature is fixed at 100°C (see Section 2.1) there are two degrees of freedom ($k_la$ and either $UA$ or $T_{\mathrm{cool}}$). Table 3 defines a base case ($k_la$, $UA$, $T_{\mathrm{cool}}$) and the corresponding desired steady state, which exists but is not necessarily stable.

The objective of this study is to investigate the dynamic behaviour and the stability of the hydroformylation reactor and the influence of the cooler ($UA$, $T_{\mathrm{cool}}$) and the mass transfer ($k_la$) on this. This is achieved by investigation of the steady state conditions, by creating stability maps using the bifurcation analysis described in Section 2.3 and by simulating the process in time for various conditions.

### 3.2. Steady-state utilization, saturation and conversion

The cooling parameters ($UA$ and $T_{\mathrm{cool}}$) can influence the stability of the steady state(s). However, since the reaction temperature is fixed at 100°C, $UA$ or $T_{\mathrm{cool}}$ do not influence the existence and component concentrations of the steady state(s). As a consequence, the steady-state conditions are a function of the mass transfer ($k_la$) only.

Fig. 2 (Table 4) shows the saturation, utilization and conversion as a function of $k_la$. It can be seen that the liquid phase is not saturated for $k_la$ values below about $1\,\mathrm{s}^{-1}$. Despite this, the conversion stabilises at a maximum of about 52% for $k_la = 0.035\,\mathrm{s}^{-1}$ and above. This is quite unusual for gas–liquid reactors, because within

Table 1
System definition (reaction and physical parameters)

| | |
|---|---|
| Absorption | $H_2(g) \rightarrow H_2(l)$ |
| with | $CO(g) \rightarrow CO(l)$ |
| reaction | $H_2(l) + CO(l) + \mathrm{olefin}(l) \rightarrow \mathrm{aldehyde}(l)$ |
| Reaction rate | See Eq. (2) |
| $k_{R0}$ | 50,000 |
| $E_{\mathrm{act}}$ | 60,000 J mol$^{-1}$ |
| $R$ | 8.314 J mol$^{-1}$ K$^{-1}$ |
| $K_{\mathrm{CO}}$ | 0.05 |
| $K_{\mathrm{H_2}}$ | 0.5 |
| $\Delta H_R$ | $-100{,}000$ J mol$^{-1}$ |
| $m_{\mathrm{H_2}}$ | 0.075 |
| $m_{\mathrm{CO}}$ | 0.175 |
| $\rho_l$ | 1000 kg m$^{-3}$ |
| $C_{P,l}$ | 2000 J kg$^{-1}$ K$^{-1}$ |

Table 2
System definition (fixed operating conditions)

| | |
|---|---|
| $k_g$ | 100 m s$^{-1}$ (no gas resistance) |
| $\varepsilon_l$ | 0.15 |
| $V_R$ | 1.0 m$^3$ |
| $P_{\mathrm{H_2}}$ | 5 bar |
| $P_{\mathrm{CO}}$ | 5 bar |
| $\Phi_{l,\mathrm{in,out}}$ | $1.0 \cdot 10^{-4}$ m$^3$ s$^{-1}$ |
| [cat] | 0.5 mol m$^{-3}$ |
| $[\mathrm{olefin}]_{l,\mathrm{in}}$ | 6000 mol m$^{-3}$ |
| $[H_2]_{l,\mathrm{in}}$ | 0.0 mol m$^{-3}$ |
| $[CO]_{l,\mathrm{in}}$ | 0.0 mol m$^{-3}$ |
| $T_{l,\mathrm{in}}$ | 373.15 K (100°C) |

Table 3
Base case settings and desired steady state

| | |
|---|---|
| $k_la$ | 0.1 s$^{-1}$ |
| $UA$ | 1000 WK$^{-1}$ |
| $T_{\mathrm{cool}}$ | 342.0 |
| $T_l$ | 373.15 K (100°C) |
| $[\mathrm{olefin}]_l$ | 2867 mol m$^{-3}$ |
| $[H_2]_l$ | 9.1 mol m$^{-3}$ |
| $[CO]_l$ | 24.8 mol m$^{-3}$ |
| $[\mathrm{aldehyde}]_l$ | 3133 mol m$^{-3}$ |
| $\zeta$ | 0.52 |
| $\eta$ | 1.07 |
| $\eta_{\mathrm{H_2}}$ | 0.76 |
| $\eta_{\mathrm{CO}}$ | 0.88 |

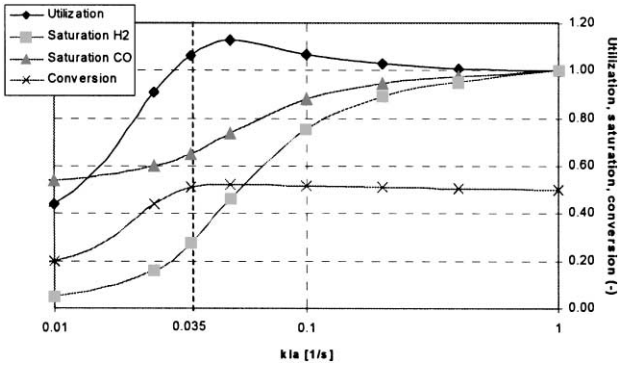


Fig. 2. Utilization (Eq. (25)), saturation (Eq. (24)) and conversion for the conditions given in Tables 1–3 versus the mass transfer coefficient $k_l a$. Kinetics controlled regime.

Table 4
Data of Fig. 2 ($E_{a,H_2} = 1.0$ and $E_{a,CO} = 1.0$ for all conditions)

| $k_l a$ $(s)^{-1}$ | $\eta_{H_2}$ | $\eta_{CO}$ | $\eta$ | $\zeta$ | Stability map |
|---|---|---|---|---|---|
| 0.01 | 0.05 | 0.54 | 0.44 | 0.20 | |
| 0.025 | 0.16 | 0.60 | 0.91 | 0.44 | Fig. 3a |
| 0.035 | 0.27 | 0.65 | 1.07 | 0.52 | Fig. 3b |
| 0.05 | 0.46 | 0.74 | 1.13 | 0.52 | Fig. 3c |
| 0.1 | 0.76 | 0.88 | 1.07 | 0.52 | Fig. 3d |
| 0.2 | 0.89 | 0.95 | 1.03 | 0.51 | |
| 0.4 | 0.95 | 0.98 | 1.01 | 0.51 | |
| 1.0 | 1.00 | 1.00 | 1.00 | 0.50 | |

the kinetics controlled regime, the maximum conversion is usually obtained when the liquid phase is saturated. This unusual phenomenon is caused by the negative reaction order of CO. Apparently, the increasing $H_2$ and CO concentrations cancel each other out and the overall reaction rate (Eq. (2)) remains unchanged.

From the calculations, performed using the rigorous model, it was clear that for all conditions, the enhancement factor of both $H_2$ and CO is equal to 1.0. Therefore, the assumption made by using Eq. (23) in the approximate model is allowed.

### 3.3. Bifurcation analysis (*approximate model*)

In the previous section it was shown that from a conversion standpoint of view, the hydroformylation reactor performs the same for any value of $k_l a$ above $0.035\ s^{-1}$. The performed calculations did not however consider the static and dynamic stability of the reactor. To obtain an insight into the dynamics, stability maps are created using the bifurcation analysis and the approximate reactor model.

From the stability maps (Fig. 3), it can be seen that the unstable regions (region II and III) become larger with increasing $k_l a$. Also, the required minimum cooling capacity $UA$ for stability at an operating temperature of 100°C increases with increasing mass transfer ($k_l a$). In other words, mass transfer limitations reduce the instability without necessarily affecting the conversion. The data from some specific points in the stability maps is shown in Table 5.

If, for example, a reactor with an $UA$ of $1000\ W\,K^{-1}$ is chosen, the design is in region Ia (stable) for $k_l a = 0.025\ s^{-1}$ (Fig. 3a), in region Ib (stable) for $k_l a = 0.035\ s^{-1}$ (Fig. 3b) and in region II (dynamic unstable) for $k_l a > 0.05\ s^{-1}$ (Fig. 3c and d). The design with the lowest mass transfer ($0.025\ s^{-1}$) has the largest stability but a lower conversion (44% versus 52%). Therefore, the reactor with $k_l a = 0.035\ s^{-1}$ is the best choice is this case: it is stable and has a high conversion (52%).

### 3.4. Dynamic system behaviour

From the stability analysis, it was predicted that different types of dynamic system behaviour could be expected for the hydroformylation reactor, depending on the mass transfer and the cooling coefficient (see Fig. 3 and Table 5). This has been analysed in more detail by solving both the rigorous and the approximate reactor model in time for some specific conditions. All cases were chosen so that the same steady state (conversion 52% and temperature 100°C) exists, but it is not necessarily stable.

Fig. 4 shows the reactor temperature in time for $k_l a = 0.1\ s^{-1}$ and four different values of $UA$, ranging from 500 to 4000 $WK^{-1}$. The results correspond with the predictions shown in the stability map of Fig. 3d. The differences between the results found by the rigorous model and the approximate model are small. The small differences are caused by the fact that with the increasing temperature the assumption $E_a = 1$, made in the approximate model, is no longer valid.

The specific case with $k_l a = 0.1\ s^{-1}$ and $UA = 1000\ WK^{-1}$ is analysed more detailed in Fig. 5. The limit cycles of the liquid-phase olefin, $H_2$ and CO concentrations versus the temperature are plotted. From this figure, it is very clear that the system never reaches the steady state, which is also indicated in the figure. The system is dynamically unstable for $k_l a = 0.1\ s^{-1}$.

However, if $k_l a$ is decreased to $0.035\ s^{-1}$, the limit cycle vanishes and the system becomes stable. The corresponding spiral point is shown in Fig. 6.

## 4. Conclusions

A rigorous and an approximate model are presented that can describe the dynamic behaviour of an ideally stirred hydroformylation reactor (two-phase CISTR).

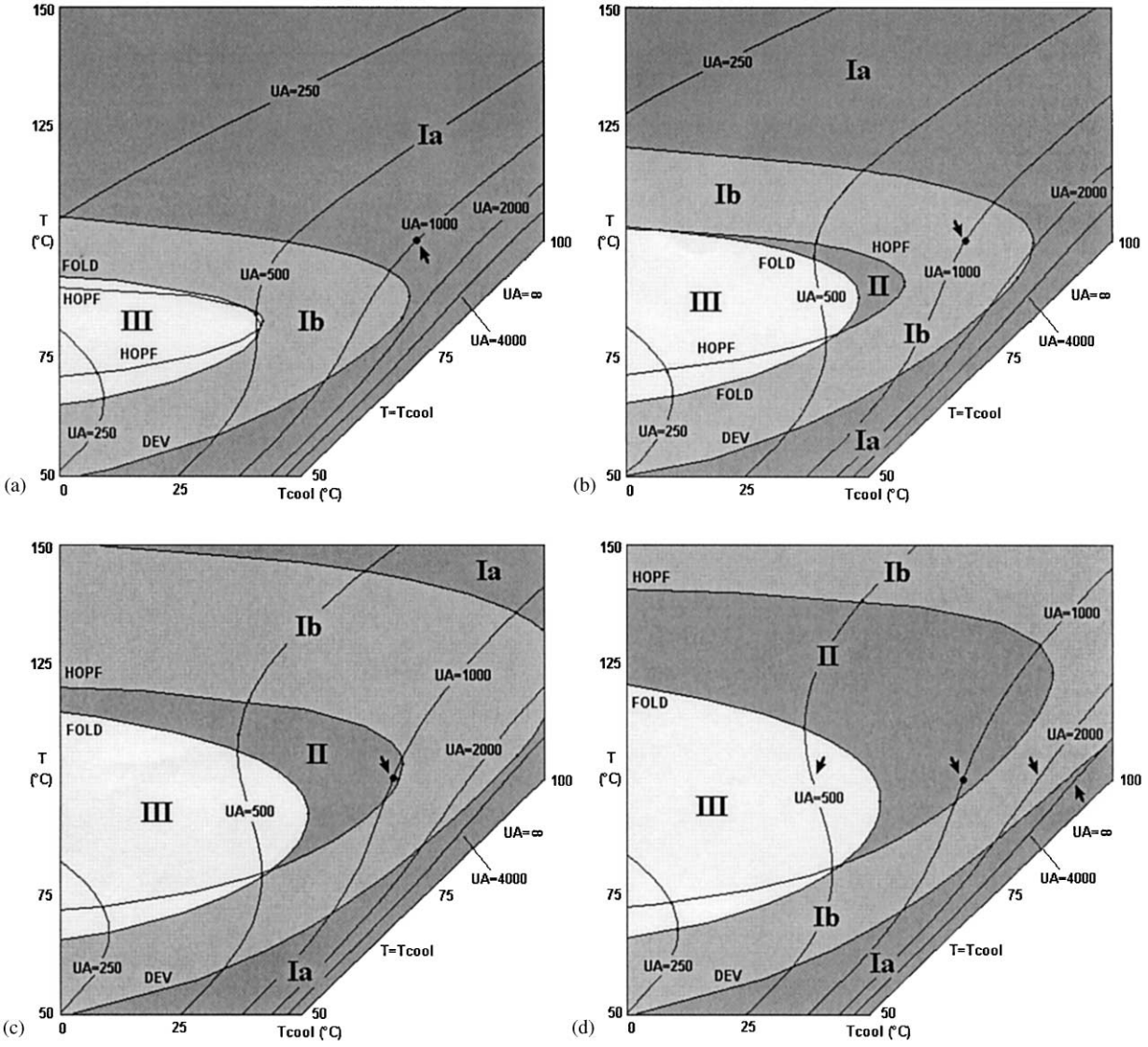


Fig. 3. Stability maps for different values of $k_l(a)$. Valid in kinetics controlled regime. See Fig. 1 for an explanation about the dynamics in the different regions. (a) Stability map for $k_l a = 0.025\ s^{-1}$. $UA = 1000\ WK^{-1}$ and $T = 100°C$ in region Ia (point stable), conversion 44% (Fig. 2), (b) in region Ib (spiral point), conversion 52% (Fig. 2), (c) in region II (limit cycle), conversion 53% (Fig. 2), (d) in region II (limit cycle), conversion 52% (Fig. 2).

Table 5
Summary of specific points from the stability maps in Fig. 3

| $k_l a$ ($s^{-1}$) | $UA$ ($WK^{-1}$) | $T_{cool}$ (K) | $T_l$ (K) | $\zeta$ | Dynamics | Figures |
|---|---|---|---|---|---|---|
| 0.025 | 1000 | > 342.0 | 373.2 | 0.44 | Asymptotic damping | 3a |
| 0.035 | 1000 | 342.0 | 373.2 | 0.52 | Spiral point | 3b, 6 |
| 0.05 | 1000 | 342.0 | 373.2 | 0.52 | Limit cycle | 3c |
| 0.1 | 1000 | 342.0 | 373.2 | 0.52 | Limit cycle | 3d, 4b, 5 |
| 0.1 | 500 | 310.7 | 373.2 | 0.52 | Static unstable | 3d, 4a |
| 0.1 | 1000 | 342.0 | 373.2 | 0.52 | Limit cycle | 3d, 4b, 5 |
| 0.1 | 2000 | 357.6 | 373.2 | 0.52 | Spiral point | 3d, 4c |
| 0.1 | 4000 | 365.5 | 373.2 | 0.52 | Asymptotic damping | 3d, 4d |

The rigorous model is valid over the entire range of conditions ranging from kinetics controlled pre-mixed feed to mass transfer controlled infinitesimal fast reaction (see Westerterp, van Swaaij, & Beenackers, 1990). The approximate model is, due to Eq. (23), only valid in the kinetics controlled regime ($E_a = 1$). The approximate model is however very useful for performing stability analysis.

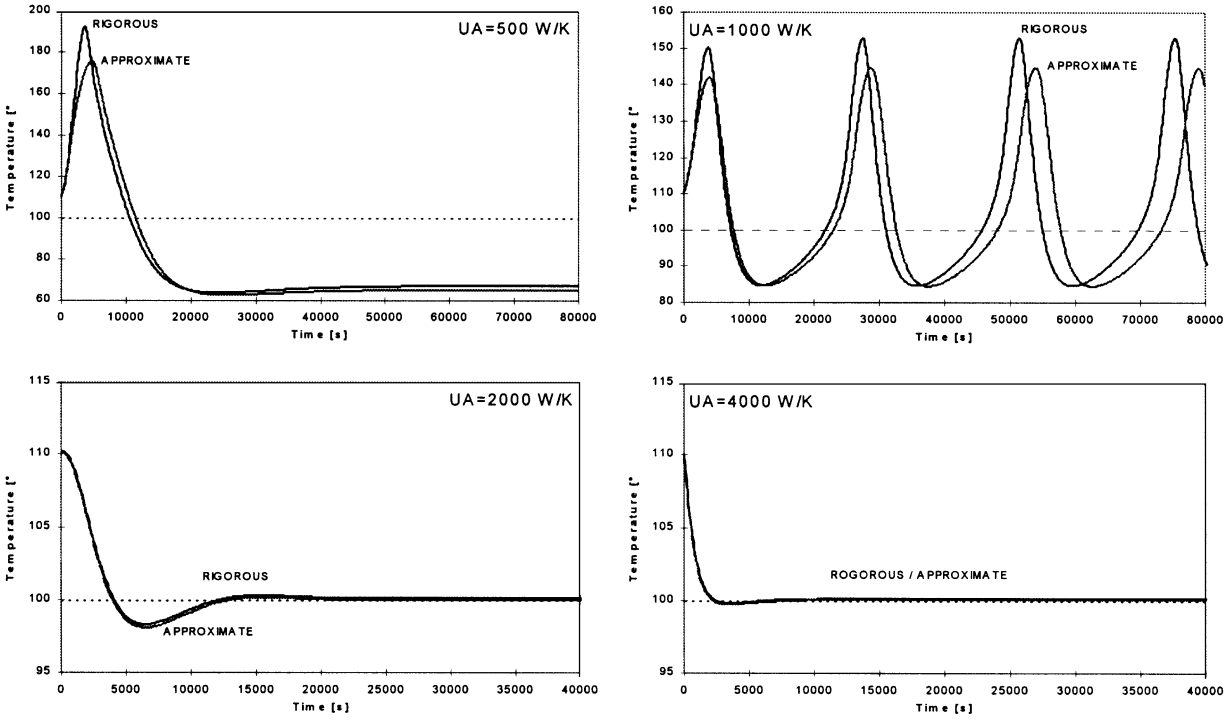


Fig. 4. Dynamic system behaviour at $k_l a = 0.1\ s^{-1}$ and a steady state at 100°C for various values of the cooling coefficient $UA$ after a step disturbance of 10°C. At $UA = 500\ WK^{-1}$, the system is in region III (transition), at $UA = 1000\ WK^{-1}$, the system is in region II (limit cycle), at $UA = 2000\ WK^{-1}$, the system is in region Ib (spiral point) and at $UA = 4000\ WK^{-1}$, the system is in region Ia (asymptotic damping). See also stability map of Fig. 3d and the schematic presentation of Fig. 1.

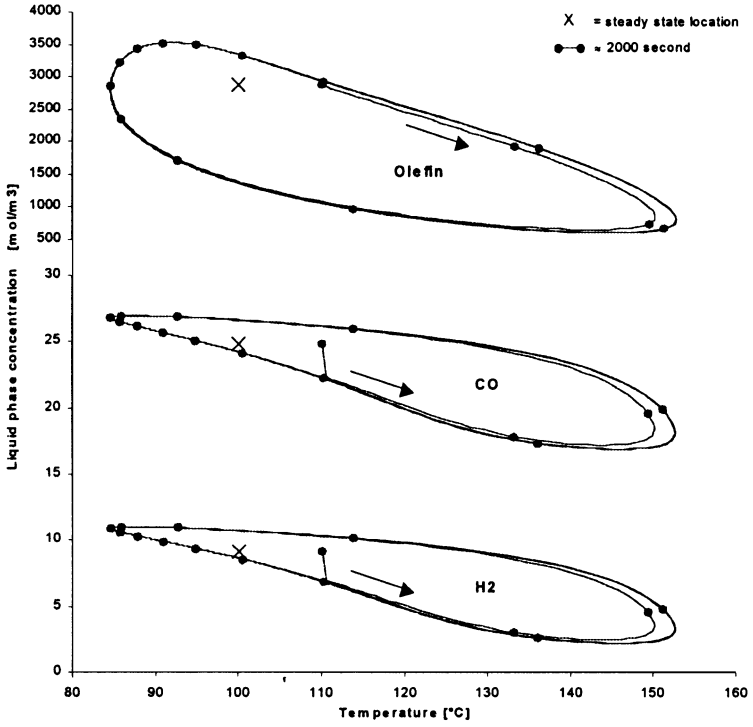


Fig. 5. Limit cycle for $k_l a = 0.1\ s^{-1}$ and $UA = 1000\ WK^{-1}$ and a steady state at 100°C. The various liquid-phase concentrations are plotted versus the reactor temperature. Steady-state conversion 52%, see also Fig. 2.

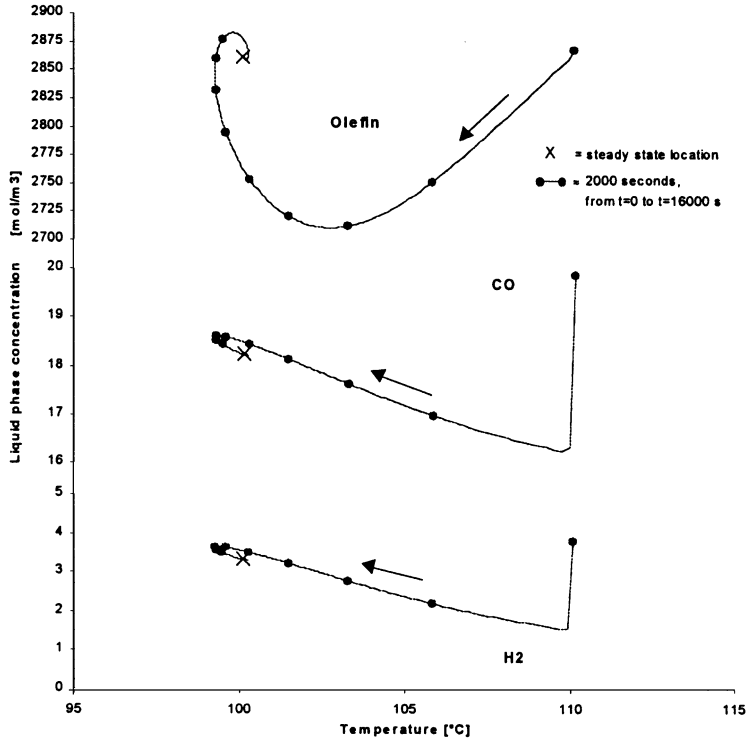


Fig. 6. Spiral point for $k_l a = 0.035\ s^{-1}$ and $UA = 1000\ WK^{-1}$ and a steady state at 100°C. The various liquid-phase concentrations are plotted versus the reactor temperature. Steady-state conversion 52%, see also Fig. 2.

With the rigorous model it was found that (see Fig. 2), for the specific system considered, the conversion is almost independent of $k_l a$ for $k_l a$ larger than $0.035\ s^{-1}$. Below a $k_l a$ of $0.035\ s^{-1}$, the conversion drops with decreasing $k_l a$. This is common for gas–liquid reactors, once the system is saturated $k_l a$ has no influence on the performance. The specific system considered in the current work is however not saturated at $k_l a = 0.035\ s^{-1}$ but at $k_l a$ above about $1.0\ s^{-1}$. This unusual phenomenon is caused by the negative reaction order of CO. Apparently, the increasing $H_2$ and CO concentrations cancel each other out, so that the overall reaction rate remains unchanged.

From the stability analysis, using the approximate reactor model, it is concluded that the specific system considered in this study could show dynamically unstable behaviour (limit cycle) for certain specific conditions. The system becomes more stable if the mass transfer ($k_l a$) is decreased or the cooling coefficient ($UA$) is increased (see Fig. 3).

Combining the two preceding conclusions, it can be said that for the considered system the optimal $k_l a$ is about $0.035\ s^{-1}$. Lower values of $k_l a$ decreases the conversion and larger values make the system less stable. This unusual phenomenon is again caused by the negative reaction order of CO.

## Notation

| | |
|---|---|
| $a$ | specific contact area, $m^2\ m^{-3}$ |
| $A$ | heat transfer area, $m^2$ |
| $C_P$ | heat capacity, $J\ kg^{-1}\ K^{-1}$ |
| $D_{\text{subscript}}$ | diffusivity, $m^2\ s^{-1}$ |
| $E_{\text{act}}$ | activation energy, $J\ mol^{-1}$ |
| $E_{a,\text{subscript}}$ | enhancement factor, l |
| $h$ | heat transfer coefficient, $W\ m^{-2}\ K^{-1}$ |
| $h_{\text{ov}}$ | overall heat transfer coefficient (defined by $h_g h_l/(h_g + h_l)$, $W\ m^{-2}\ K^{-1}$ |
| $\Delta H_R$ | heat of reaction based on R, $J\ mol^{-1}$ |
| $J_{\text{subscript}}$ | molar flux, $mol\ m^{-2}\ s^{-1}$ |
| $k$ | mass transfer coefficient, $m\ s^{-1}$ |
| $k_R$ | reaction rate constant |
| $m_{\text{subscript}}$ | gas–liquid partition coefficient, l |
| $R$ | reaction rate, $mol\ m^{-3}\ s^{-1}$ |
| $R_{gas}$ | ideal gas constant, $J\ mol^{-1}\ K^{-1}$ |
| $t$ | simulation time variable, s |
| $T$ | temperature, K |
| $U$ | heat transfer coefficient, $W\ m^{-2}\ K^{-1}$ |
| $V_R$ | reactor volume, $m^3$ |
| $[\,]$ | concentration, $mol\ m^{-3}$ |
| $[\,]_{\text{subscript}}$ | concentration, $mol\ m^{-3}$ |

*Greek letters*

| | |
|---|---|
| $\varepsilon$ | hold-up, l |
| $\rho$ | density, kg m$^{-3}$ |
| $\theta$ | contact time according to penetration model (defined by $4D_a/\pi k_l^2$), s |
| $\tau$ | residence time, s |
| $\xi_{\text{subscript}}$ | absolute conversion, mol |
| $\zeta$ | relative conversion, l |

*Subscripts*

| | |
|---|---|
| 0 | initial value |
| bulk | at bulk conditions |
| cool | cooling medium |
| $g$ | gas phase |
| $i$ | interface |
| in | at inlet conditions |
| $l$ | liquid phase |
| ov | overall |
| ss | steady state value |
| $T$ | temperature |

## Acknowledgements

The investigations were supported by DSM Research Geleen.

## References

van Elk, E.P., Borman, P. C., Kuipers, J. A. M., & Versteeg, G. F. (2000). Modelling of gas–liquid reactors — implementation of the penetration model in dynamic modelling of gas–liquid processes, *Chemical Engineering Journal*, *76*, 223–237.

van Elk, E. P., Borman, P. C., Kuipers, J. A. M., & Versteeg, G. F. (1999). Modelling of gas–liquid reactors — stability and dynamic behavior of gas–liquid mass transfer accompanied by irreversible reaction. *Chemical Engineering Science*, *45*, 4869–4879.

Heiszwolf, J. J., & Fortuin, M. H. (1997). Design procedure for stable operations of first-order reaction systems in a CSTR. *A.I.Ch.E. Journal*, *43*, 1060–1068.

Higbie, R. (1935). The rate of absorption of a pure gas into a still liquid during short periods of exposure. *Transactions of the American Institute of Chemical Engineering*, *35*, 36–60.

Huang, D. T.-J., & Varma, A. (1981a). Steady-state and dynamic behavior of fast gas–liquid reactions in non-adiabatic continuous stirred tank reactors. *Chemical Engineering Journal*, *21*, 47–57.

van Swaaij, W. P. M. ., & Versteeg, G. F. (1992). Mass transfer accompanied with complex reversible chemical reaction in gas–liquid systems: an overview. *Chemical Engineering Science*, *47*, 3181–3195.

Vleeschhouwer, P. H. M., Garton, R. D., & Fortuin, J. M. H. (1992). Analysis of limit cycles in an industrial oxo reactor. *Chemical Engineering Science*, *47*, 2547–2552.

Westerterp, K. R., van Swaaij, W. P. M., & Beenackers, A. A. C. M. (1990). Chemical reactor design and operation. New York: Wiley.